Available online at www.sciencedirect.com
SCIENCE DIRECT®
PERGAMON
Continental Shelf Research 23 (2003) 991–1003
CONTINENTAL SHELF RESEARCH
www.elsevier.com/locate/csr

Eddies around Guam, an island in the Mariana Islands group

E. Wolanski[a,*], R.H. Richmond[b], G. Davis[c], E. Deleersnijder[d], R.R. Leben[e]

[a] *Australian Institute of Marine Science, PMB No. 3 MC, Townsville, Qld. 4810, Australia*
[b] *Marine Laboratory, University of Guam, UOG Station, Mangilao, Guam 96923, USA*
[c] *Division of Aquatic and Wildlife Resources, Guam Department of Agriculture, Mangilao, Guam 96923, USA*
[d] *G. Lemaitre Institute of Astronomy and Geophysics, Catholic University of Louvain, Chemin du Cyclotron 2, B-1348 Louvain-la-Neuve, Belgium*
[e] *Colorado Center for Astrodynamics Research, University of Colorado, Boulder, CO 80309-0431, USA*

Received 4 June 2002; accepted 14 April 2003

Abstract

Near-surface currents around Guam, a 35 km long, slab-shaped island in the Mariana Islands group, were estimated from current meters, satellite-derived surface topography, and a numerical model. A dominant northwestward-flowing North Equatorial Current prevailed from June to December 2000, with speeds typically 0.1–0.2 m s^{-1}, generating unsteady eddies in the lee of Guam. A number of transient eddies off the tips of the island were apparent, the smallest eddies were at the scale of local topographic features such as headlands and embayments, while other eddies were island size. In addition to eddies off the tips of the island, a large (200 km in diameter) cyclonic oceanic eddy was advected eastward past Guam during the last 2 weeks of August 2000. Centered on Guam for a few days, this eddy formed elsewhere and impinged on the island generating anticlockwise currents around the island of up to 0.5 m s^{-1}. It is suggested that these eddies are sufficiently energetic to return fish and coral eggs and larvae to their natal reefs in Guam, thereby enabling self-seeding of coral reefs in Guam. The numerical model also predicts that large (up to 30 m amplitude) island-generated internal waves may occur around Guam; however, no observations are presently available to support this prediction.

Keywords: Eddies; Oceanic islands; North Equatorial Current; Altimetry; Coral reefs; Guam

1. Introduction

The general ocean circulation around Guam (144°50′E, 13°20′N; Fig. 1), Mariana Islands in the Western Pacific Ocean, is little known. This 50 km long, slab-shaped island is oriented about southwest to northeast. The shelf is very narrow, the 180 and 360 m depth contours are found at a few km offshore. A number of coastal strips that include fringing coral reefs have recently been set aside as marine reserves. A key question to answer for the management of these reserves is how these are connected by oceanic drift of plankton, fish and coral larvae. This question remains unanswered because little is known about the large-scale oceanic circulation around Guam, and how the island locally modifies this circulation. Given that the overall flow is northwestward (Uda, 1970),

*Corresponding author. Tel.: +61-77-534243; fax: +61-77-725852.
E-mail address: e.wolanski@aims.gov.au (E. Wolanski).

0278-4343/03/$ - see front matter © 2003 Elsevier Ltd. All rights reserved.
doi:10.1016/S0278-4343(03)00087-6

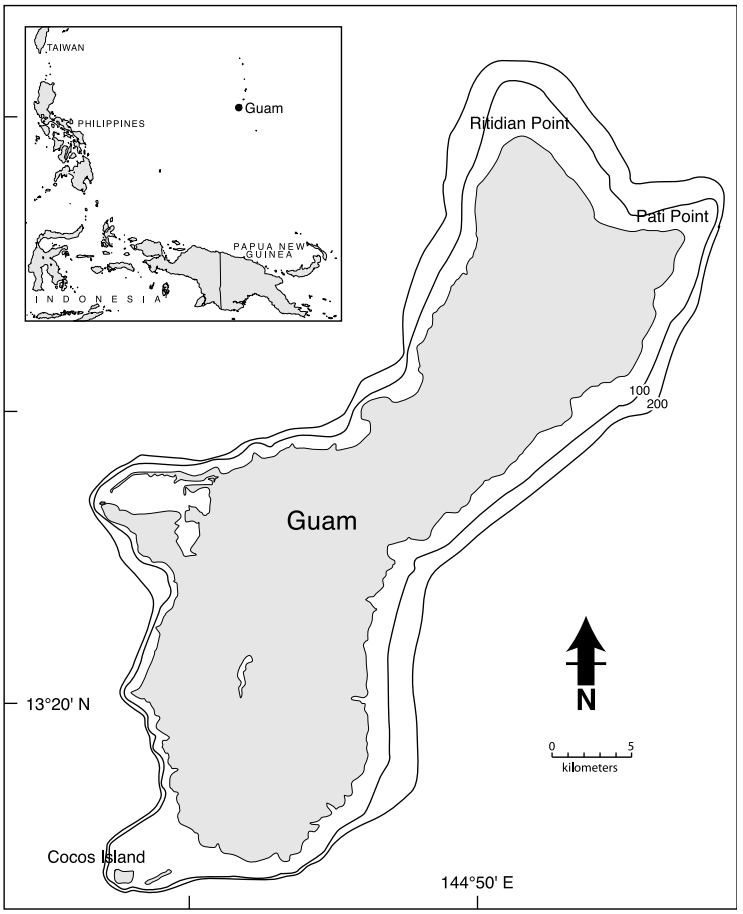

Fig. 1. The inset shows a location map of Guam in the Mariana Island group. Bathymetric map of Guam showing the three key capes, which, as discussed in the text, may act as separation points. Depth in fathoms (1 fathom = 1.8 m).

Guam has three salient capes that could steer the currents and generate eddy motions, namely Pati Point and Ritidian Point in the North, and Cocos Island in the South.

Island-generated eddies or return flows may recirculate eggs and larvae of coral reef fishes (Sale, 1970; Lobel, 1981; Boehlert et al. 1992; Cowen and Castro, 1994; Tyler and Sanderson, 1996; Heywood et al., 1996; Carleton et al., 2001; Rodriguez et al., 2001; Seki et al., 2001). Oceanic islands do not always generate eddies from headlands (Wolanski and Deleersnijder, 1998; Harlan et al., 2002). Large-scale oceanic features that originate elsewhere, such as oceanic eddies which impinge on the island, may also exist and return fish and coral eggs and larvae to their natal reefs (Lee et al., 1994; Cowen et al., 2000).

The large-scale oceanic circulation around Guam is controlled by the North Equatorial current flowing northwestward at about 0.1–0.2 m s^{-1} (Uda, 1970). Recently, TOPEX/Poseidon satellite altimetry analyses show that the large-scale circulation fluctuates in speed (peaking at 0.3 m s^{-1}) and in direction (from northward to westward), and may have reversed direction in June 1997 during an El Nino event (Lagerloef et al., 1999; see also www.esr.org and coastwatch.nmfs.hawaii.edu/cwatch/docs/satelite.html). There are no long-term current meter data from this area; however, there was a NOAA Wx buoy

west of Guam that collected weather data only through 1994 (www.ndbc.noaa.gov). The Coast Guard SAR abandoned ship drift prediction model has a grid resolution larger than the size of Guam and hence does not predict a blocking effect by Guam's landmass. This blocking effect is apparent in the trajectory of people lost at sea to the west of Guam, some were trapped in small eddies in the lee of the island and were not advected away by the prevailing northwestward North Equatorial Current (G. Davis, unpublished data).

Near-surface currents measured from satellite altimetry and current meters are presented in this paper. Combined with a numerical model of the circulation around Guam, it is shown that both island-generated eddies as well as large-scale oceanic eddies prevail. These eddies may retain and return eggs and larvae to Guam's fringing coral reefs. In addition, the model suggests that large-scale (up to 30 m amplitude) island-generated internal waves may exist around Guam.

2. Methods

2.1. Current metering

Three sets of data are available. Firstly, a RDI Workhorse ADCP was bottom mounted at about 18–22 m depth for about a tidal cycle at sites shown in Fig. 2, both west and south of Pati Point from July 25 to August 14, 2000. Secondly, current meter data at site D (see location map in Fig. 3a) were obtained for 8 months in 1969–1970 by Jones and Randall (1971). Thirdly, current meter data were collected for periods lasting between typically 1 week to 1 month at sites A–C and E–K in 1971 (see location map in Fig. 3a; see Table 1 for details of data duration).

2.2. Drifter data

The data set comprises the trajectories of eight drifting fish aggregation devices that had a surface buoy, a chain and rope going down to about 100 m depth after the drifters were set adrift by shark attacks at the level of the thermocline (at about 100 m depth). All data were collected under normal trade-wind conditions. The position of each drifter was obtained daily, usually at about 1300 h, by the US Coast Guard. See Table 2 for details.

2.3. Satellite altimetry

A blended TOPEX/POSEIDON and ERS satellite altimeter data product for mapping mesoscale circulation (Leben et al., 2002) was used to monitor the mesoscale oceanic circulation surrounding Guam. Maps were made every 3 days from the available data at a resolution of 0.25° in a $2^\circ \times 2^\circ$ study domain centered on the island.

2.4. Numerical model

A two-layer, non-linear model was used to predict the interaction of the observed prevailing oceanic currents with the landmass of Guam. The far-field open boundary conditions are poorly defined and the current data are so sparse that no detailed comparisons can be made. A two-layer model is well suited to schematically represent the interaction of currents with an island in a stratified ocean. The model uses the radial coordinates $(r;\theta)$ and the following equations:

Continuity equations

$$\frac{\partial H_i}{\partial t} = -\frac{1}{r}\frac{\partial (rU_i)}{\partial r} - \frac{1}{r}\frac{\partial V_i}{\partial \theta} \quad (i = 1, 2).$$

Radial momentum equations

$$\frac{\partial U_i}{\partial t} = -\frac{1}{r}\frac{\partial}{\partial r}\left(ru_iU_i - Ar\frac{\partial U_i}{\partial r}\right) - \frac{1}{r}\frac{\partial}{\partial \theta}\left(v_iU_i - \frac{A}{r}\frac{\partial U_i}{\partial \theta}\right) + \frac{v_iV_i}{r} + fV_i - gH_i\frac{\partial e_i}{\partial r} \quad (i = 1, 2).$$

Zonal momentum equations

$$\frac{\partial V_i}{\partial t} = -\frac{1}{r}\frac{\partial}{\partial r}\left(ru_iV_i - Ar\frac{\partial V_i}{\partial r}\right) - \frac{1}{r}\frac{\partial}{\partial \theta}\left(v_iV_i - \frac{A}{r}\frac{\partial V_i}{\partial \theta}\right) - \frac{u_iV_i}{r} - fU_i - \frac{gH_i}{r}\frac{\partial e_i}{\partial \theta} \quad (i = 1, 2).$$

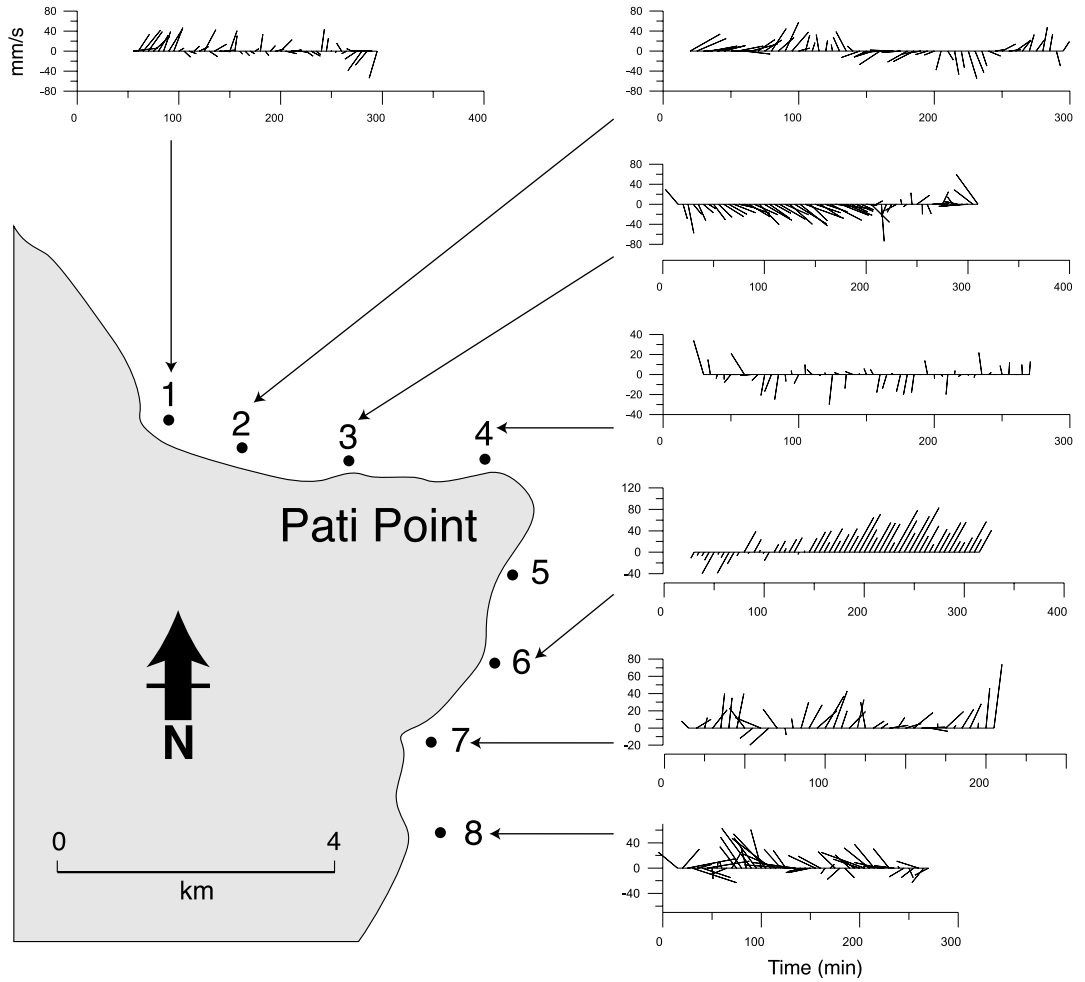

Fig. 2. Details of the coastline around Pati Point (see a location map in Fig. 1), showing the location of mooring points and time series of current shown as stick plots. Velocity in mm s^{-1}.

In these equations, subscripts 1 and 2 refer to the top layer and the bottom layer, respectively, h_1 (=constant) is the unperturbed thickness of the top layer=constant, $h_2(r,\theta)$ is the unperturbed thickness of the bottom layer, $\eta(t,r,\theta)$ is the displacement of the ocean surface (>0 if upward), $\xi(t,r,\theta)$ is the displacement of the pycnocline (>0 if upward), $H_1(=h_1+\eta-\xi)$ is the actual thickness of the top layer, $H_2(=h_2+\xi)$ is the actual thickness of the bottom layer. The density in the ith layer is $\rho_i(i=1,2)$, the relative density difference is $\varepsilon=\rho_2-\rho_1/\rho_2$, the equivalent elevation in the top layer is $e_1=\eta$, the equivalent elevation in the bottom layer is $e_2=\eta+\varepsilon\xi$, the radial velocity in the ith layer is $u_i(t,r,\theta)\,(i=1,2)$, the zonal velocity in the ith layer is $v_i(t,r,\theta)\,(i=1,2)$, the transport is $(U_i,V_i)=H_i(u_i,v_i)\,(i=1,2)$, the eddy viscosity is $A(r)$, g is the gravitational acceleration and f is the Coriolis factor.

The island bathymetry is accurate and thus not radially symmetric. The outer radius of the model was 520 km. As shown in Fig. 4, there were 46 grid points selected along a radial, which were unevenly spaced so that maximum resolution was achieved near the island. The angular resolution was 6°. The ocean was divided in two layers vertically,

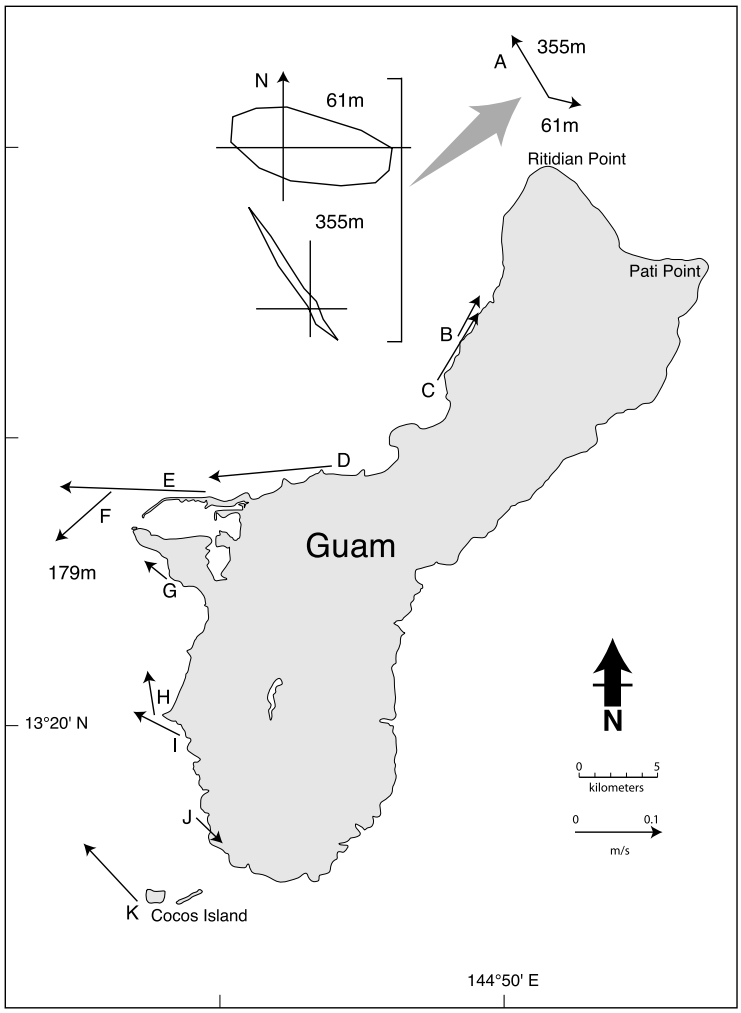

(a)

Fig. 3. (a) Net currents, shown as arrows, at 11 sites in coastal waters of Guam. The inset shows the directional histograms of currents. The histograms represent the variability about the mean, and have the same velocity scale. See Table 1 for mooring details. (b) Trajectory at daily intervals, of eight drifters labelled 1–8. See Table 2 for details.

each of constant density. The surface layer was assumed to be 120 m thick at 26°C and the bottom layer was 18°C. The salinity was uniform. No tangential stress was assumed to occur at the interface between the two layers. A linear friction stress was assumed on the sea floor. The eddy viscosity varied linearly from about $3\,m^2\,s^{-1}$ at the island boundary to about $300\,m^2\,s^{-1}$ at the open boundary of the computational domain to account for increased sub-grid-scale dispersion with increasing grid size (Okubo, 1974). The model was forced by a net sea-level gradient so as to generate a uniform current in the far field of the island. The sea-level gradient was adjusted so that the modeled far-field current reproduced the far-field current observed by satellite altimetry. There was no explicit forcing of the internal wave at the open boundary where a sponge layer was added to absorb all outgoing wave energy.

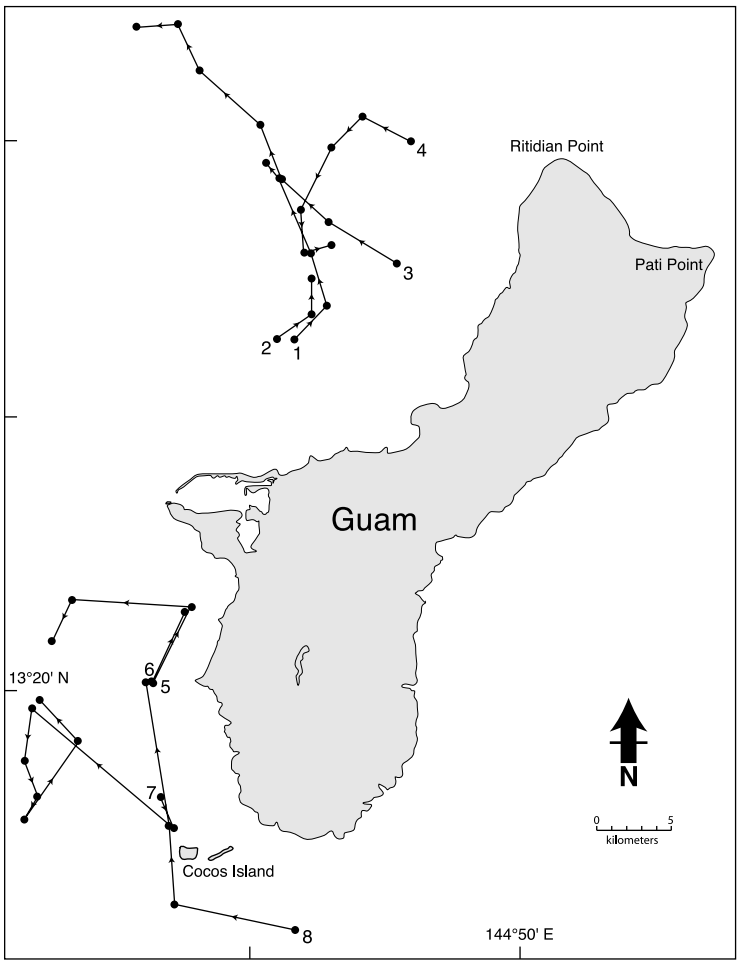

(b)

Fig. 3 (*continued*).

Table 1
Oceanographic mooring data used in Fig. 3a

Site	Water depth (m)	Current meter depth (m)	Time	Source
A	400	61 and 355	August 25–September 13, 1971	Huddell et al. (1974)
B	100	17	August 22–September 12, 1971	Huddell et al. (1974)
C	33	31	August 22–September 12, 1971	Huddell et al. (1974)
D	18	16	October 1969–July 1970	Jones and Randall (1971)
E	18	16	August 22–September 12, 1971	Huddell et al. (1974)
F	925	179	September 3–14, 1971	Huddell et al. (1974)
G	22	20	August 22–September 9, 1971	Huddell et al. (1974)
H	22	19	August 21–September 9, 1971	Huddell et al. (1974)
I	17	15	August 28–September 9, 1971	Huddell et al. (1974)
J	66	17	August 21–September 9, 1971	Huddell et al. (1974)
K	32	30	August 28–September 9, 1971	Huddell et al. (1974)

Table 2
Characteristics of the drifter trajectory data shown in Fig. 3b

Trajectory number	Initial time	Last time
1	0700 h, April 4, 1988	1400 h, April 11, 1988
2	1500 h, July 20, 1995	1000 h, July 22, 1995
3	1200 h, December 14, 1987	1100 h, December 20, 1987
4	0800 h, August 17, 1990	0900 h, August 21, 1990
5	1600 h, September 6, 1990	1200 h, September 10, 1990
6	1300 h, May 2, 1996	0900 h, May 5, 1996
7	1500 h, January 23, 1989	1000 h, January 30, 1989
8	1600 h, August 3, 1987	1100 h, August 6, 1987

Data are shown at daily intervals. The drifters were fish aggregation devices that had a surface buoy, a chain and rope going down to about 100 m depth after the drifters were set adrift by shark bites at the level of the thermocline (at about 100 m depth). All data were collected under normal tradewind conditions, no data during storms are presented.

3. Results

3.1. Current meter data

The small tides (typically 0.5 m) in Guam introduced weak tidal currents peaking at about $0.05\,m\,s^{-1}$ near Pati Point (Fig. 2) and $0.08\,m\,s^{-1}$ in offshore waters (site A in Fig. 3a). Around Pati Point in July–August 2000, the net currents nearshore were eastward at $0.06\,m\,s^{-1}$ to the west of Pati Point and northward to the south of Pati Point (Fig. 2).

A net northwestward current at $0.08–0.1\,m\,s^{-1}$ prevailed near the leading edges of Guam, namely from August 28 to September 9, 1971 near Cocos Island near the surface (site K in Fig. 3a), and from August 25 to September 13, 1971 near Ritidian Point (site A) at 355 m depth. However, net currents at 61 m depth at site A were half as strong and eastward; the currents were much more variable at 61 m depth than at 355 m depth (see the current histogram in Fig. 3a). There appears to be a separation point between sites C and D to the west of Guam, with a northward circulation along the coast north of site C and a westward circulation along the coast west of site D. These westward currents form a convergence near site F, with northward currents prevailing to the south of site F. Smaller coastal eddies may also exist near site J where a southward current was observed. At any site, net currents were usually less than 0.1 m s

3.2. Drifter data

To the northwest of Guam, the data for drifter No. 4 (Fig. 3b) suggest a current oriented towards site C. A northwestward drift was apparent for drifters No. 1–3.

A westward current of $0.1\,m\,s^{-1}$ was observed south of Cocos Island for drifters No. 7 and 8 (Fig. 3b). Eddy motions in the lee of Guam prevailed for drifters No. 5 and 7. Drifter No. 7 returned within less than 1 km from its original position after 5 days. Currents in the eddies varied between 0.03 and $0.08\,m\,s^{-1}$. A northward coastal current prevailed at $0.02–0.07\,m\,s^{-1}$, in agreement with the current meter data further inshore (Fig. 3a).

3.3. Satellite-derived near-surface currents

The large-scale oceanic currents upstream of Guam (at 13°N, 145°E) fluctuated mainly between northward to northwestward (Fig. 5), at speed averaging about $0.18\,m\,s^{-1}$. These dominant currents were interrupted during the last 2 weeks of August 2000 by strong eastward to southeastward currents peaking at $0.5\,m\,s^{-1}$. The synoptic distribution (Fig. 6, for June 2, 2000) during the typical northwestward current shows fairly uniform far-field currents with speeds of about $0.1\,m\,s^{-1}$, with corresponding sea-level variations (not shown) not exceeding a few cm in the $2^\circ \times 2^\circ$ domain. The August flow reversal event was caused by the passage of a cyclonic oceanic eddy with a dimension of about 1.7° and a water-level depression of about 25 cm at the center. This oceanic eddy came from the southwest and moved northeastward towards Guam, and was centered over Guam on day 208, at which time it generated

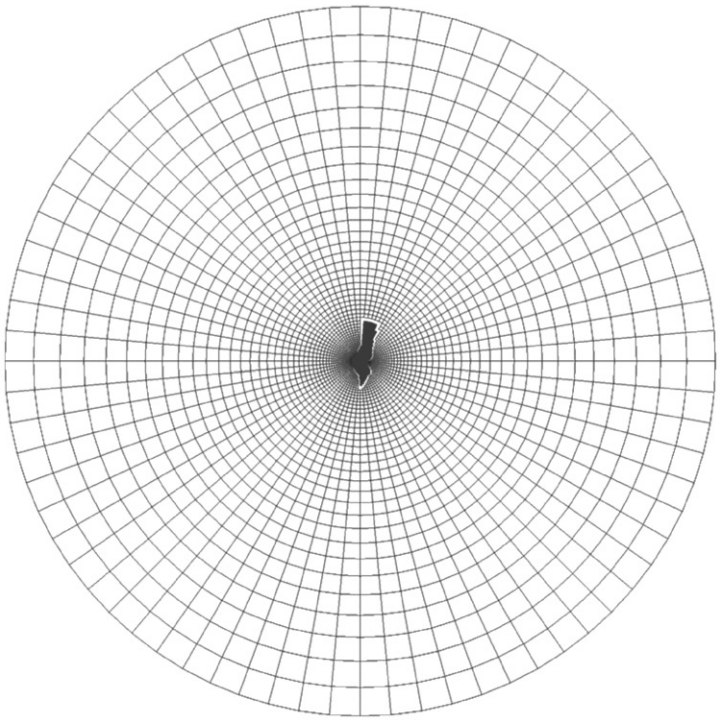

Fig. 4. Model grid.

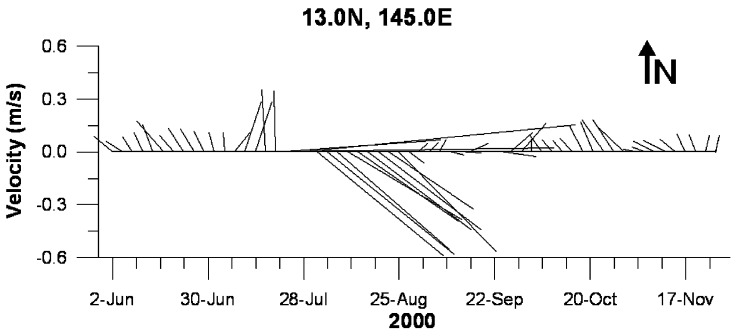

Fig. 5. Time series plot in June–December 2000, of near-surface currents shown as stick plots at 13°N, 145°E, as measured from satellite altimetry from TOPEX/Poseidon. North is up the page.

a strong (peaking at about $0.5\,m\,s^{-1}$) northwestward current to the North of Guam and southeastward current South of Guam (Fig. 6, for June 29, 2000). The eddy then decreased in size while moving eastward (day 238; Fig. 6, for July 11, 2000) and disappeared from the study domain by day 241. Thereafter, the normal northwestward current was re-established (Fig. 5).

3.4. Numerical model

When the prevailing oceanic current is steady and oriented west-northwestward, the model predicts (Fig. 7) unsteady eddy shedding in the lee of Guam. In the North, a large, sluggish, cyclonic eddy is predicted to be shed from Ritidian Point. This eddy generates a weak current (peak velocity

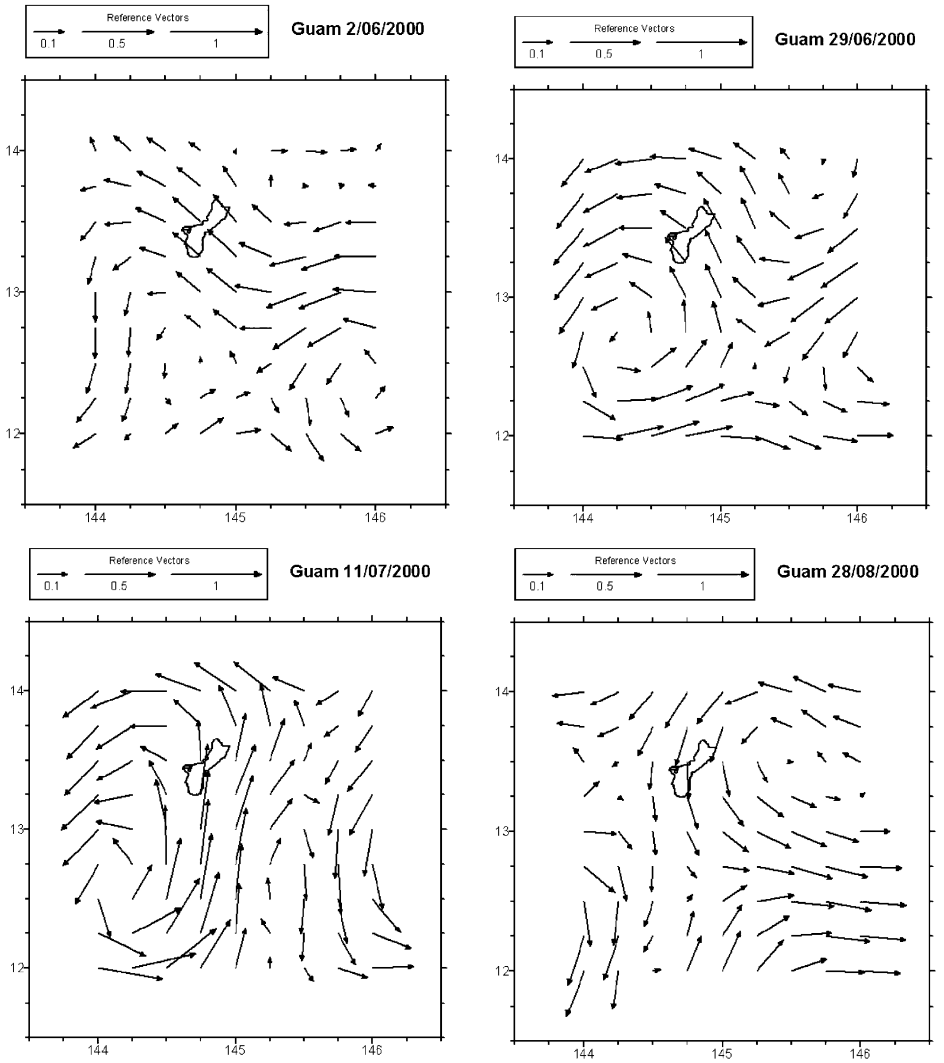

Fig. 6. Examples of the synoptic distribution during the second half of 2000 of the synoptic distribution of near-surface currents ($m\,s^{-1}$) in a $2^\circ \times 2^\circ$ domain centered around Guam, as derived from satellite altimetry data from TOPEX/Poseidon. The island in the middle is Guam.

of a few $cm\,s^{-1}$) along the northwest coast of Guam. In the south, vortices are predicted to be periodically shed from Cocos Island. These vortices move westward, away from Guam. Water from the northern, large, sluggish eddy is entrained in these smaller, more intense eddies in the south.

When the prevailing flow is northwestward to westward, the model predicts that the two separation points are Cocos Island in the South and Pati Point to the North (Fig. 8). Unsteady anticyclonic eddies are shed from Cocos Island and travel northwestward, while a small eddy is predicted to be shed from Pati Point and to extend from Pati Point to Ritidian Point. This eddy is predicted to be locked between Pati Point and Ritidian Point, it does not move away, and generates an eastward coastal flow to the west of Pati Point. The flow at the same time is predicted to be northward to the south of Pati Point. The currents near Ritidian

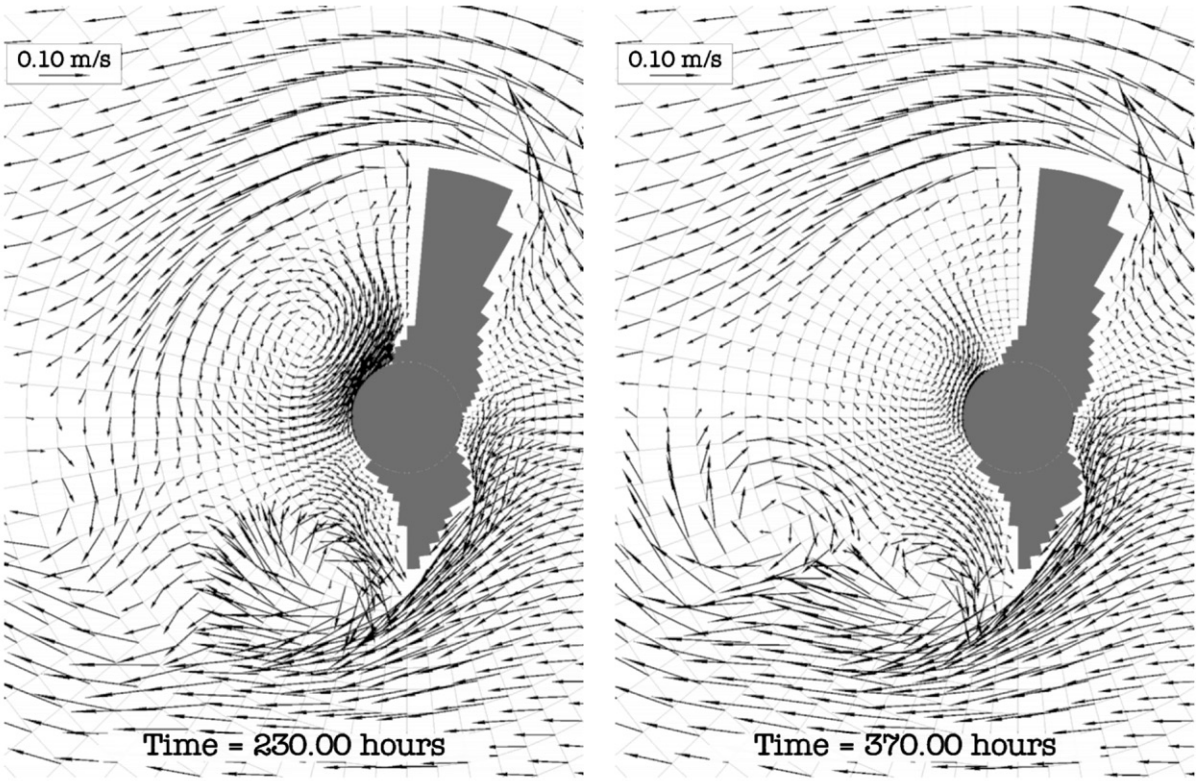

Fig. 7. Two examples of the predicted synoptic distribution of the predicted near-surface currents around Guam for a west-northwestward far-field current impinging on Guam.

Point are sluggish and a stagnation zone prevails near this headland. These three predictions are in qualitative agreement with the observations.

Similarly to that reported at Scott Reef, Western Australia (Wolanski and Deleersnijder, 1998), an island-generated internal wave is predicted to exist around Guam. The predicted wave is 180° out-of-phase across the island, with the wave trough and the wave crest located on opposite sides of the island, and it propagates clockwise around Guam in about 4 days. The wave may oscillate the thermocline by up to 60 m peak to trough around Guam. The thermocline displacement is predicted to be largest along the island slopes and decreases with increasing distance from the island. Energy is dissipated as free internal waves radiating away from the island. It is not known if the thermocline around Guam may be weakened close to the island by vertical mixing (Simpson et al., 1982). The more gradual stratification would support weaker oscillations. No data are available to validate these predictions.

4. Discussion

The circulation around the island of Guam is spatially and temporally variable. The data are not synoptic; indeed some were obtained in different years, which makes data interpretation tentative.

Our current meter data are also sparse and limited to a few days of data in coastal waters near Pati Point, a headland in the northeast of Guam. These data suggest a prevailing northward flow, with a peak current of $0.06\,m\,s^{-1}$ along the east coast of the island and a return flow to the west of Pati Point. This circulation has been widely reported by divers (G. David, unpublished data).

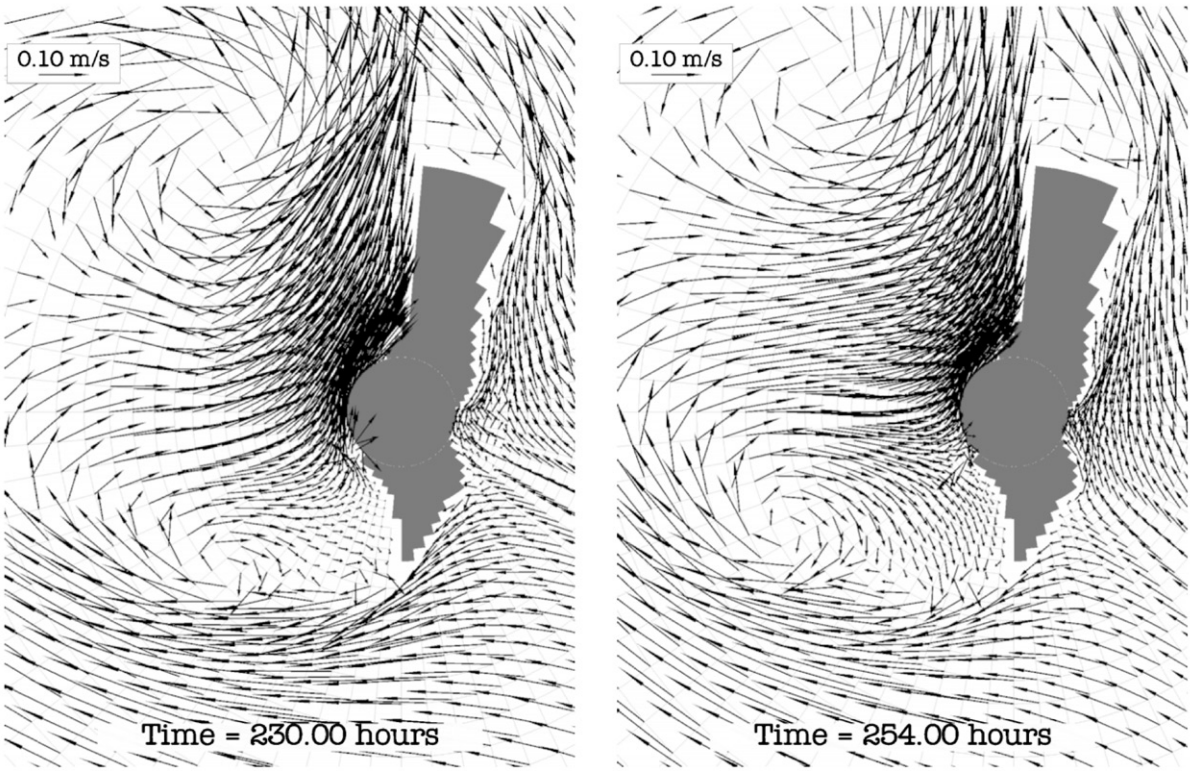

Fig. 8. Two examples of the predicted synoptic distribution of the predicted near-surface currents around Guam for a northwestward far-field current impinging on Guam.

Longer time series of current meter data, but always less than 1 month in duration, are available in coastal waters at 11 sites along the west coast of Guam. These data suggest an oceanic inflow in the lee of Guam between sites C and D. On meeting the coast this inflow apparently divided into two coastal currents, namely a northward flow north of site C and a westward flow west of site B. This westward current converged with a northward current to the south of site F.

One drifter to the northwest of Guam also suggests a net, weak oceanic inflow toward site C. The drifters also show the presence of a northwestward current further north, in which eddies were imbedded.

To the south of Guam, the drifter data show a westward current at speed of $0.1\,m\,s^{-1}$. To the southwest of Guam, the data show energetic, cyclonic eddies with a complete rotation in 4–5 days.

The satellite altimetry data offer a glimpse of the large-scale surface currents impinging on the island of Guam. Based on the data from June to December 2000, most of the time the current is homogenous at the scale of the island. The dominant current fluctuates from westward to northward typically at speeds of $0.1–0.2\,m\,s^{-1}$. This finding justifies the use of a local area model with uniform flow in the far field to study the likely surface circulation near Guam. Such a model is needed because the resolution of the altimetry data is too coarse to resolve the circulation around Guam for periods when the far-field current impinging on the island is homogeneous. There was one period when such a model would not be valid, namely the last 2 weeks of August 2000, when a 200 km wide cyclonic eddy generated elsewhere drifted past the island and impinged on the island. For a few days during that period the eddy was centered on the island, generating an

anticlockwise circulation around Guam with peak currents of about $0.5\,m\,s^{-1}$.

For the periods when the far-field oceanic current was homogenous, the model predicts a complex flow field in the lee of Guam. The three dominant capes of Guam (Cocos Island to the South, and Ritidian Point and Pati Point to the North) act as eddy-shedding separation points. The finding of an unsteady eddy in the lee of Guam generated by the North Equatorial Current may be similar to the finding by Mitchum (1995) that the North Equatorial Current generated eddies off the tip of the Island of Hawaii. In Hawaii however, cold-core eddies are also formed as a result of trade winds and the high topography (Seki et al., 2001). Possibly, the island of Guam may not have sufficient topography to generate such eddies.

The circulation in the lee of Guam generated by the interaction of the North Equatorial Current with the island mass, is predicted to be strongly dependent on the precise angle the far-field current impinges on the island. Three types of eddies result, namely intense vortices shed from Cocos Island, a sluggish, island-size eddy in the northwest with an oceanic inflow toward site C, and a small, stationary eddy located between Ritidian Point and Pati Point. The data are too sparse, and non-synoptic, for a quantitative verification of the model. The model predictions, however, are in qualitative agreement with the findings from the drifter data and current meter data. These eddies are suppressed in the model if higher values ($>300\,m^2\,s^{-1}$) of the eddy diffusion coefficient are selected (Heywood et al., 1996). Such high values, however, may be unrealistic here because our model resolves horizontal scales less than 1 km and time scales on the order of minutes; the value of the eddy diffusion increases with increasing horizontal and temporal scales (Fischer et al., 1979).

The model also predicts that a large-amplitude island-generated internal wave may exist around Guam. There are no observations to support this prediction; however, similar waves have been observed in other Oceanic islands, namely Tahiti in French Polynesia (Wolanski and Delesalle, 1995), Mururoa and Fangataufa atolls in French Polynesia (Garrigues et al., 1993) and Scott Reef in Western Australia (Wolanski and Deleersnijder, 1998). This mechanism may be biologically important in that it provides an episodic upwelling of nutrient-rich sub-thermocline waters to coral reefs. The three-dimensional circulation generated by these internal waves also provides a mechanism for pre-settlement fish larvae to adjust their behavior and swimming depth to remain near a reef (Cowen and Castro, 1994).

The scope of our study was limited. Nevertheless, we suggest the prevalence of both oceanic and island-generated eddies around Guam. These eddies are biologically important because they provide a mechanism for the trapping and return of eggs and larvae of coral and fish on Guam coral reefs, and because they control the connectivity among various reefs along the island. During northwestward flow, the topographic eddy between Ritidian Point and Pati Point may ensure self-seeding of local reefs, and much of Cocos Island coral spawn may drift away at sea, though some may return near point C. During west-northwestward flow, much of Cocos Island coral spawn may drift away at sea; however, spawn from reefs on the north coast may seed reefs along the northwest coast of Guam. The reverse situation may prevail during the passage of an oceanic eddy. Data are unavailable to estimate the relative frequency of these various processes.

Because these mechanisms of self-seeding and connectivity are crucial for the sustainability of Guam's coral reefs and for the management of marine reserves, more detailed studies of the water circulation especially during coral spawning, are warranted.

Acknowledgements

The University of Guam, Guam Department of Agriculture, the Australian Institute of Marine Science, and the US EPA STAR program supported this study. Support has also been provided by NASA contract 1221120. Eric Deleersnijder is a Research Associate with the National Fund for Scientific Research of Belgium (FNRS). It is a

pleasure to thank V. Bonito, S. Spagnol, R. Deiotte and P. Gimeno.

References

Boehlert, G.W., Watson, W., Sun, L.C., 1992. Horizontal and vertical distributions of larval fishes around an isolated oceanic island in the tropical Pacific. Deep-Sea Research 39, 439–466.

Carleton, J.H., Brinkman, R., Doherty, P.J., 2001. The effects of water flow around coral reefs on the distribution of pre-settlement fish (Great Barrier Reef, Australia). In: Wolanski, E. (Ed.), Oceanographic Processes of Coral Reefs. Physical and Biological Links in the Great Barrier Reef. CRC Press, Boca Raton, FL, pp. 209–230.

Cowen, R.K., Castro, L.R., 1994. Relation of coral reef fish larval distributions to island scale circulation around Barbados, West Indies. Bulletin of Marine Science 45 (1), 228–244.

Cowen, R.K., Lwiza, K.M.M., Sponaugle, S., Paris, C.B., Olson, D.B., 2000. Connectivity of marine populations: Open or closed? Science 287 (N5454), 857–859.

Fischer, H.B., List, E.J., Koh, R.C.Y., Imberger, J., Brooks, N.H., 1979. Mixing in Inland and Coastal Waters. Academic Press, New York, 483pp.

Garrigues, L., Deleersnijder, E., Rancher, J., 1993. Modelisation bi-dimensionelle a deux couches de la circulation autour des iles. Application aux atolls de Fangataufa et Mururoa. Service Mixte de Securite Radiologique, Monthery, France, 85pp.

Harlan, J.A., Swearer, S.E., Leben, R.R., Fox, C.A., 2002. Surface circulation in a Caribbean island wake. Continental Shelf Research 22, 417–434.

Heywood, K.J., Stephens, D.P., Bigg, G.R., 1996. Eddy formation behind the tropical island of Aldabra. Continental Shelf Research 43, 55–73.

Huddell, H.D., Willet, J.C., Marchand, G., 1974. Nearshore Currents and Coral Reef Ecology of the West Coast of Guam, Mariana Islands. Naval Oceanographic Office, Washington, DC, 185pp.

Jones, R.S., Randall, R.H., 1971. An annual cycle study of biological, chemical and oceanographic phenomena associated with the Agana ocean outfall. University of Guam Marine Laboratory, Mangilao, Guam, Technical Report No. 1, 67pp.

Lagerloef, G.S.E., Mitchum, G.T., Lukas, R.B., Niller, P.P., 1999. Tropical Pacific near-surface currents estimated from altimeter, wind, and drifter data. Journal of Geophysical Research 104 (C10), 23313–23326.

Leben, R.R., Born, G.H., Engebreth, B.R., 2002. Operational altimeter data processing for mesoscale monitoring. Marine Geodesy 25, 1–21.

Lee, T.N., Clarke, M.E., Williams, E., Szmant, A.F., Berger, T., 1994. Evolution of the Tortugas gyre and its influence on recruitment in the Florida keys. Bulletin of Marine Science 54 (3), 621–646.

Lobel, P.S., 1981. Ocean current variability and the spawning season of Hawaiian fish larvae. Environmental Biology of Fishes 24, 161–171.

Mitchum, G.T., 1995. The source of 90-day oscillation at Wake Island. Journal of Geophysical Research 100, 2459–2475.

Okubo, A., 1974. Some speculations on oceanic diffusion diagrams. Rapport des Proces-Verbaux des Reunions du Conseil International pour l'Exploration de la Mer 167, 77–85.

Rodriguez, J.M., Barton, E.D., Hernandez-Leon, S., 2001. Mesozooplankton and ichthyoplankton distribution around Gran Canaria, on oceanic island in the NE Atlantic. Deep-Sea Research I 48, 2161–2183.

Sale, P.F., 1970. Distribution of larval acanthuridae off Hawaii. Copeia 1970, 765–766.

Seki, M.P., Polovina, J.P., Brainard, R.E., Bidigare, R.R., Leonard, .C.L., Foley, D.G., 2001. Biological enhancement at cyclonic eddies tracked with GOES thermal imagery in Hawaiian waters. Geophysical Research Letters 28, 1583–1586.

Simpson, J.H., Tett, P.B., Argotte-Spinoza, M.L., Edwards, M., Jones, K.J., Savidge, G., 1982. Mixing and phytoplankton growth around an island in a stratified sea. Continental Shelf Research 1, 15–31.

Tyler, R.H., Sanderson, B.G., 1996. Wind-driven pressure and flow around and island. Continental Shelf Research 16, 469–488.

Uda, M., 1970. Fishery oceanographic studies of frontal eddies and transport associated with the Kuroshio system including the "Subtropical Counterpart". In: Marr, J.C. (Ed.), The Kuroshio, A Symposium on the Japan Current. East-West Center Press, University of Hawaii, Honolulu, pp. 593–604.

Wolanski, E., Deleersnijder, E., 1998. Island-generated internal waves at Scott Reef, Western Australia. Continental Shelf Research 18, 1649–1666.

Wolanski, E., Delesalle, B., 1995. Upwelling by internal waves, Tahiti, French Polynesia. Continental Shelf Research 15, 357–368.